Supplementary Information

Time-resolved microfluidic flow cytometer for decode ng luminescence lifetimes in the microsecond region

Yan Wang[1,2], Nima Sayyadi[1,3], Xianlin Zheng[1,2], Travis A. Woods[4], Robert C. Leif[5], Bingyang Shi[1,6], Steven W. Graves[4], James A. Piper[1,2], Yiqing Lu[1,2,7,*]

[1]*ARC Centre of Excellence for Nanoscale BioPhotonics (CNBP),* [2]*Department of Physics and Astronomy,* [3]*Department of Molecular Sciences,* [6]*Department of Biomedical Sciences,* [7]*School of Engineering, Macquarie University, Sydney, New South Wales 2109, Australia*

[4]*Centre for Biomedical Engineering, University of New Mexico, Albuquerque, New Mexico 87131, USA*

[5]*Newport Instruments, 3345 Hopi Place, San Diego, California 92117-3516, USA*

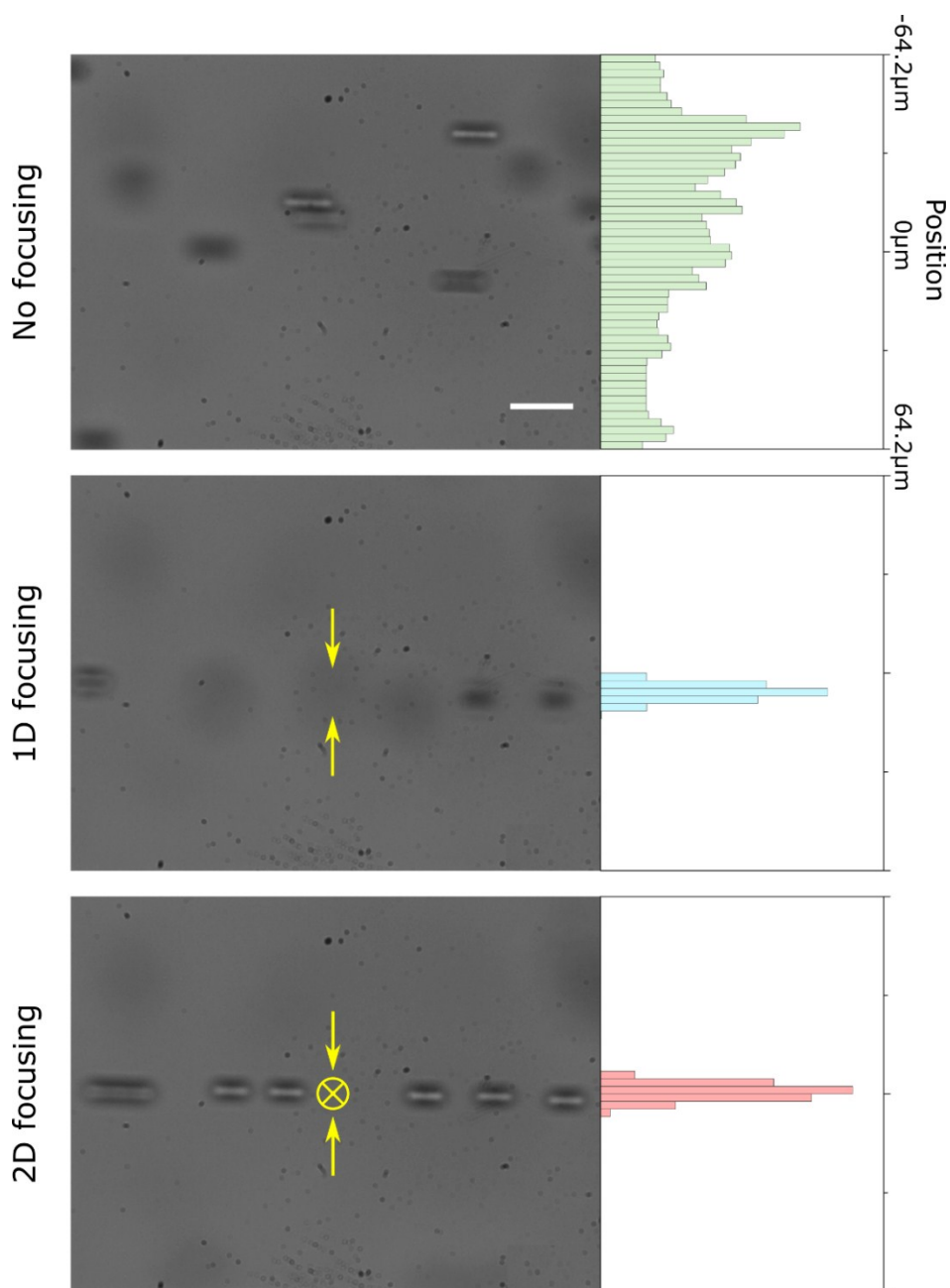[*]*Correspondence should be addressed to Y.L. (yiqing.lu@mq.edu.au)*

Contents

Figure S1 | Evaluation of acoustic focusing in the tr-mFCM using 15 μm polymer beads. The volumetric flow rate is 10 μL/min. The scale bar represents 20 μm. The histograms were each concluded from 130 video frames (taken at 26 fps) by recognising the pixels (positions) corresponding to the flowing beads using MATLAB. It can be seen that while the beads flew at random horizontal positions in the absence of acoustic focusing, they became well aligned in the middle when the piezoelectric transducer was driven at 1.272 MHz (matching the width of the channel), although many of them were out of focus. Upon FSK modulation to alternate the driving frequency between 1.272 MHz and 1.430 MHz (FSK rate 5 Hz), all the beads became both aligned in the middle and in focus.
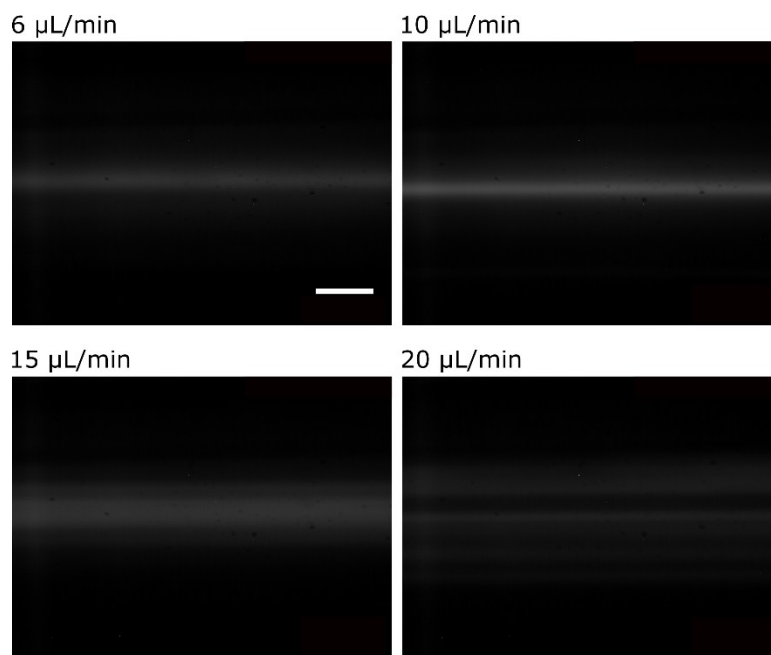
Figure S2 | The influence of flow rate on acoustic focusing, assessed in the luminescence detection model using Eu-doped microbeads. The scale bar represents 50 μm. Each image was obtained by accumulating luminescence signal for 1 minute under continuous-wave illumination of UV LED. It can be seen that the effect of acoustic focusing remains well with flow rate up to 10 μL/min, before starting to decrease as the flow rate increases further.
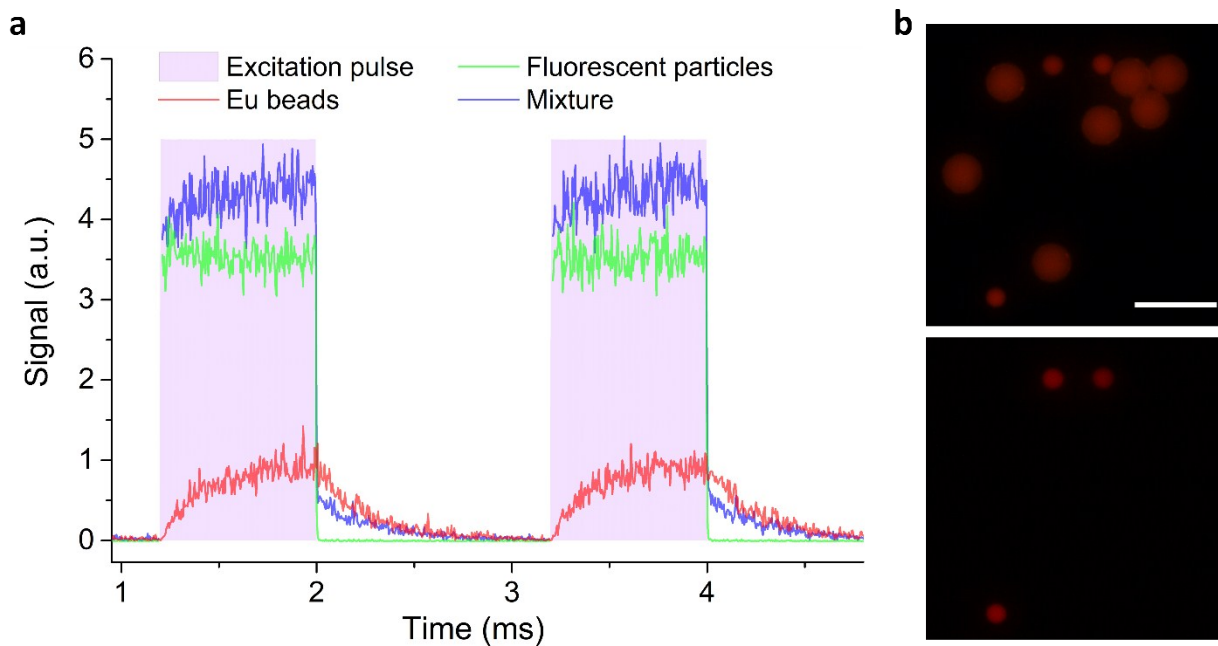
Figure S3 | Time-resolved measurements of mixed samples containing 5-µm Eu beads and 10-µm fluorescent particles. (a) The signal trains measured by tr-mFCM with pulsed excitation but no time gating. The fluorescent particles only produce signal when the excitation is on, whereas the Eu beads contribute to both on and off periods. (b) Epi-fluorescence (upper panel) and time-gated luminescence (lower panel) images of the mixture sample taken by OSAM. The Eu beads are visible in both modes, whereas the fluorescent particles are only visible in the epi-fluorescence mode but not the time-gated luminescence mode. Scale bar: 20 µm.

Note S1. Resolving of two-event overlaps

A two-event overlap can be recognised based on the number of time-gating cycles, as well as sometimes the dual peaks, in the signal trains. Figure S4 summaries the statistics of the total cycle number and peak cycle index for signal trains corresponding to single and two-overlap events. While in theory a non-overlap event should have about 90 time-gating cycles, in practice this varied between 60 to 150, due to variation in the labelling brightness and the flow velocity. By contrast, two-event overlaps typically yield over 150 cycles, with the index of second peak often beyond 100.
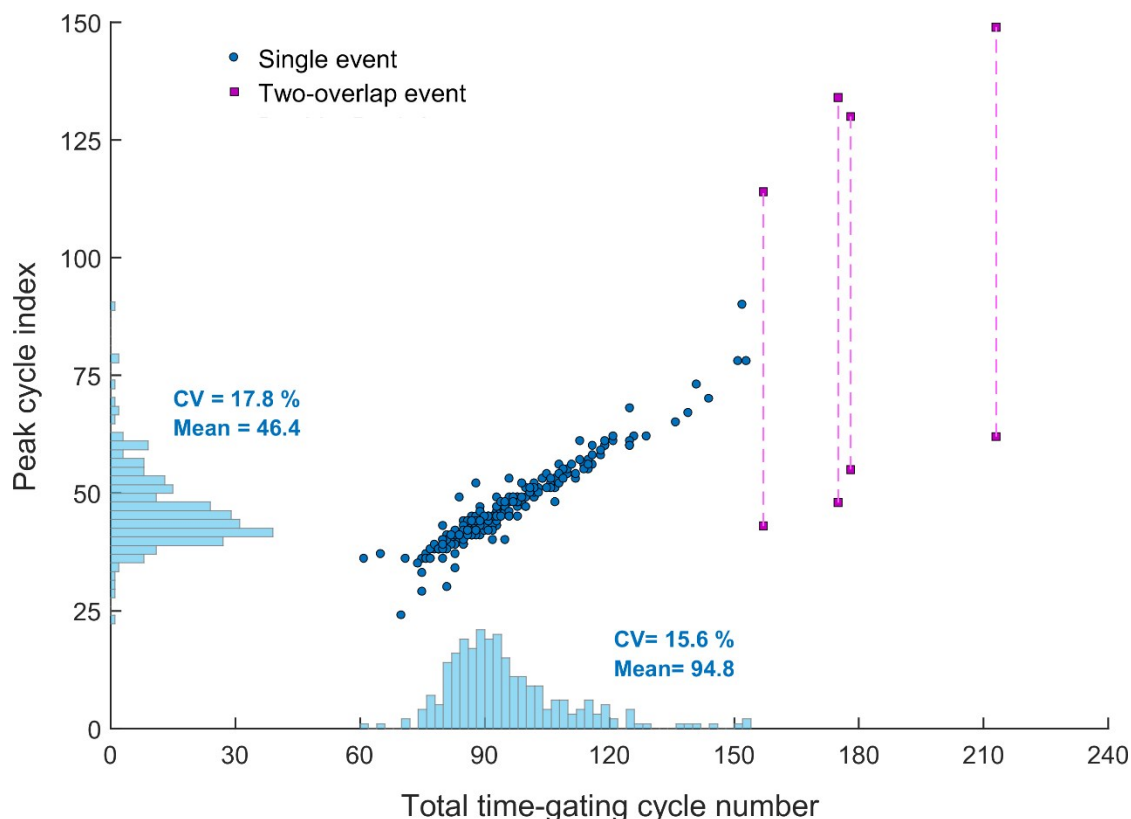

Figure S4 | Total cycle number and peak cycle index of signal trains corresponding to single and two-overlap events.

To resolve two-overlap events, we first obtained a reference profile of single event by: 1) integrating the luminescence signal among each time-gating cycles to form an envelope profile for a non-overlap event; 2) normalising the profile both in amplitude and in total cycle number; 3) averaging over many non-overlap events. The obtained "standard" profile is shown in Figure S5.
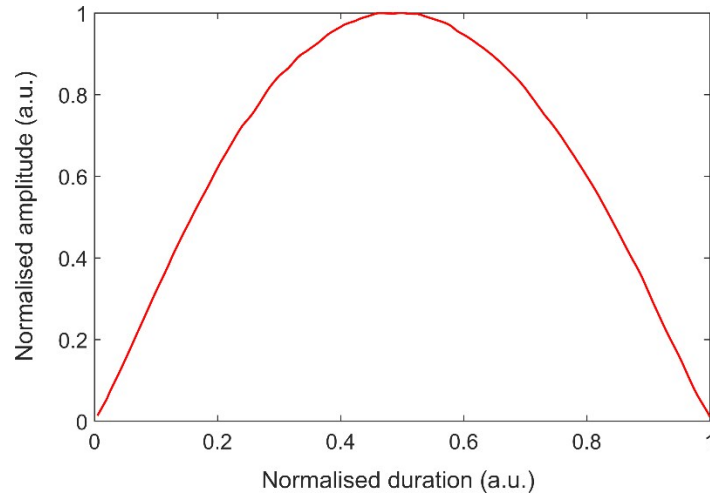
Figure S5 | Reference profile of single event.

We then assumed both events in a two-event overlap follow the standard profile, yet with variation in amplitude, duration, and time offset. If the standard profile is denoted as $F(x)$, the overall profile of the two-event overlap is given by

$$G(x) = a_1 F\left(\frac{x - b_1}{c_1}\right) + a_2 F\left(\frac{x - b_2}{c_2}\right)$$

By fitting an actual profile $G(x)$ against $F(x)$, the six variables in the above equation can be obtained and the two overlapping events resolved, as illustrated in Figure S6. Note that only fitting results with $R^2 \geq 0.95$ were accepted as successful resolving of two-overlap events, whereas the rest, possibly ascribed to three or more events occurring very close in time, were discarded.
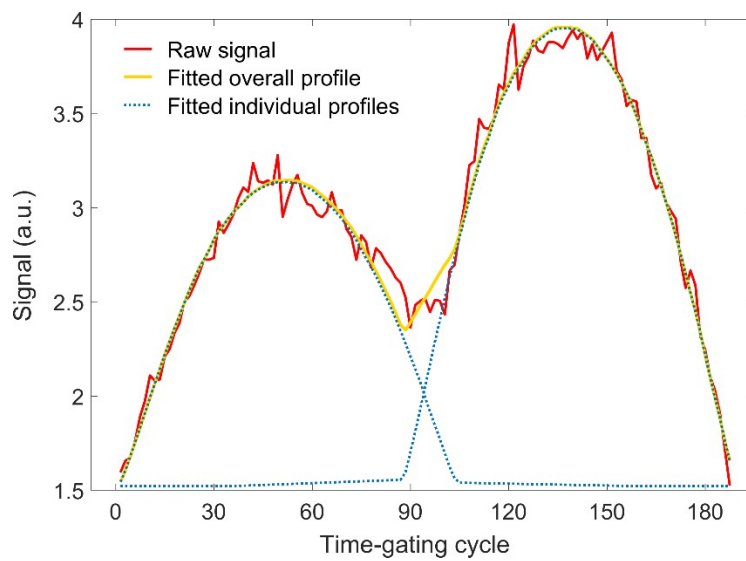

Figure S6 | Example profile fitting of a two-overlap event.

Note S2. Probability of event overlap

Assuming constant flow rate and well dispersion of the sample, the counting process for individual events (i.e. particles and/or cells) entering the detection aperture can be modelled as a homogeneous Poisson process, denoted as $\{N(t), t \geq 0\}$. The number of events appearing in a given period of time equal to the transit time T follows Poisson distribution, that is, the probability of the random variable $N(t + T) - N(t) = N(T)$ being equal to n is given by

$$P\{N(T) = n\} = \frac{(\xi T)^n}{n!} e^{-\xi T}$$

ξ is the average number of events per unit time, which is related to the sample concentration C and the volumetric flow rate Q by $\xi = CQ$. Apparently, ξ also represents the analytical throughput.

Since Q is related to the flow velocity v by $Q = Av$, where A is the cross-section area of channel, $P\{N(T) = n\}$ can also be written as

$$P\{N(T) = n\} = \frac{(CAvT)^n}{n!} e^{-CAvT} = \frac{(CAL)^n}{n!} e^{-CAL}$$

taking into account that $T = L/v$ and L is the aperture dimension. Since A is a constant, the probability of events overlap is basically determined by C and L.

Table S1 | Summary of the parameters for the tr-mFCM.

Symbol	Definition	Experimental Setting
f_H	acoustic driving frequency (horizontal)	1.272 MHz
f_V	acoustic driving frequency (vertical)	1.430 MHz
f_{FSK}	FSK frequency	5 Hz
V_{PP}	acoustic driving voltage	20 V
Q	volumetric flow rate	10 μL/min
v	flow velocity	0.55 mm/s
G_E	PMT gain	10^6
G_A	preamplifier transimpedance	10^5 V/A
T_C	time-gating period	2000 μs
T_E	excitation window	800 μs
T_W	detection window	1195 μs
T_D	time delay	5 μs
f_s	sampling rate	200 kHz
L	detection aperture	100 μm
T	standard transit time	0.18 ms
N	standard number of time-gating cycles	90
C	sample concentration	2,500 mL^{-1}
I_{th}	intensity threshold	10.0 μV·s

Table S2 | Comparison of tr-mFCM measurement of Eu beads, with and without being mixed with fluorescent particles.

Sample	Replicate	Mean Lifetime (µs)	Lifetime CV	Mean Intensity (µV·s)	Intensity CV	Counts
Eu beads only	1	250	2.3%	21	46.8%	466
	2	249	2.3%	21	40.5%	488
	3	249	2.2%	20	48.0%	533
Mixture of Eu beads and fluorescent particles	1	250	2.2%	22	47.1%	512
	2	250	2.4%	21	45.3%	492
	3	249	2.1%	21	52.6%	463